Plant Science Horizons

Research Article

Open-Access

Plant Science Horizons 2026, 1(2): e0012
https://doi.org/10.66835/psh.2026.e0012

Check for updates

Unique Regulatory Mechanism of Melatonin-Mediated Defense Against Vanadium Toxicity in *Brassica napus* L.

Latif Ullah Khan[1,2]*, Enerand Mackon[1,2], Wajid Saeed[1,2], Zhangrong Chen[1,2] Muhammad Ikram[1,2], Muhammad Umer[1,2], Yun Li[3]

[1]*School of Breeding and Multiplication, Sanya Institute of Breeding and Multiplication, Hainan University, Sanya 572025, Hainan, China.*
[2]*School of Tropical Agriculture and Forestry, Hainan University, Haikou 570228, Hainan, China.*
[3]*Guangxi Key Laboratory of Agro-Environment and Agric Products Safety, Key Laboratory of Plant Genetics and Breeding, College of Agriculture, Guangxi University, Nanning 530004, China*
***Correspondence:** latif.hainu3103@gmail.com; (Khan LU)

Abstract

Brassica napus L. (*B. napus*) is a well-known edible oil crop globally. Its production has been severely damaged by abiotic stresses, including heavy metals. Vanadium (V) is a heavy metal that can cause a reduction in plant biomass, photosynthetic pigments, and alleviate ROS production. Melatonin (MT) is a newly emerged nontoxic, regulatory bio-molecule that regulates plant growth against abiotic stresses, but there is limited knowledge about MT's mitigative role against V-induced phytotoxicity in *B. napus*. The present study investigates the MT based tolerance in *B. napus* against V toxicity by contructioing gene regulatory network by Weighted gene co-expression network analysis (WGCNA). Transcriptome profiling identified 1767 differentially expressed genes (DEGs) uniquely or commonly regulated in CK, MT, V, and MTV groups. Transcriptome-wide reprogramming at the molecular level showed that MT reduced excessive DEG fluctuations brought on by V stress, bringing expression patterns closer to the control. Cluster analyses (C2, C6) show MT-specific activation of genes involved in phenylpropanoid biosynthesis, jasmonic acid metabolism, and protein folding. WGCNA identified the black and tan modules as strongly correlated with photosynthesis, biomass, and stress traits, pinpointing hub genes *NAC072, MYB122, WRKY33, PER72, GSTU19, CYP82G1, ELF5A-2, Cox19-like, RCI2A, GRXC2, MKP1, PNSL2, CYP73A5, thioredoxin H-type, FKBP65, APR3, VHA-c5,* and *PIG-F* as central regulators of stress tolerance. These hub genes converge on redox regulation, secondary metabolism, detoxification, and hormone signaling emerging as an essential pathway. These findings advance our understanding of the mechanisms by which melatonin (MT) alleviates vanadium (V)-induced toxicity and highlight its potential as a promising approach for enhancing heavy metal stress tolerance in *B. napus*.

Keywords: Heavy Metal Stress; Vanadium; Melatonin; Transcriptome; WGCNA

Citation: Khan, L. U., Mackon, E., Saeed, W., Chen, Z., Ikram, M., Umer, M., & Li, Y. Unique regulatory mechanism of melatonin-mediated defense against vanadium toxicity in *Brassica napus* L. Plant Science Horizons 1(2): e0012 https://doi.org/10.66835/psh.2026.e0012

Introduction

The *Brassica napus* L. (*B. napus*), also known as rapeseed, is an important crop belonging to the *Brassicaceae* family. *B. napus* is the major oil-producing seed crop in China. China contributes 20% of global *B. napus* production, with 7.5 million hectares of planting area, but the edible oil self-sufficiency rate is still < 40% [1, 2]. The increasing

© The Author(s)

impact of abiotic stresses due to climate change and soil degradation poses an urgent problem for agriculture, which endangers food security in tropical and subtropical regions [3]. Crop productivity in such conditions is increasingly limited through abiotic stresses like heavy metal toxicity, high salinity, long drought, extreme pH, temperature change, and flooding that cause yield losses globally to the tune of almost 50%, far more significant than those imparted by biotic stresses [3, 4]. In this continuum, soil toxicity due to heavy metal accumulation is one of the most limiting factors for the production of sustainable agriculture in the 21st century [5, 6]. Although the proper concentrations of certain essential microelements such as Fe (iron), Cu (copper), Mo (molybdenum), Ni (nickel), Zn (zinc), Co (cobalt), and Mn (manganese) are important for plant metabolism and growth, however, their excess is toxic to plants. Typically, an overaccumulation of these elements creates imbalances in cell homeostasis, causing impaired growth with the late appearance of signs of phytotoxicity [6-8]. Among them, Vanadium (V) remains the effective poisonous heavy metal that poses an aesthetic threat to both plants and humans [7]. The V is the fifth most plentiful trace element in the Earth's crust among all the transitional elements, mainly in the USA, South Africa, and China [9]. Worldwide, the V production is 57%, China is the largest producer and user of V, which comprises around 26.5% of V-polluted soil in Southwest China [10, 11]. It is reported that about 10 to 220 mg kg^{-1} amount of V is present in the earth's crust; however, higher in human-used soils that need reduction or elimination to not transfer further to plants and food chains used by humans and animals [12, 13]. The V accumulation in various plant parts induces permanent alterations such as diminished photosynthetic activity, stomatal closure, suppressed enzymatic activities, leaf necrosis, and cellular structural damage, which ultimately reduces crop yield [14, 15]. At 35 mg L^{-1} level of V in rice and 40 mg L^{-1} in tomato, the malondialdehyde (MDA) and hydrogen peroxide (H2O2) accumulation were increased noticeably, which in turn reduced the rice growth [12, 13]. The enhanced V accumulation above the threshold level (40-55.8 mg L^{-1} causes a reduction in plant essential nutrient production, thus damaging crop yield [4, 14, 16, 17]. The increased V concentration hinders the physiological, phenotypic, and biochemical activities of plants, hence reducing the plant growth and development, mostly due to reactive oxygen species (ROS) production, alteration in enzymatic activities, and gene expression [17]. The exogenous V application (40 and 80 mg L^{-1}) significantly altered the root architecture and reduced the root and stem fresh weight and fruit production [6, 16, 18]. Similar results were obtained by Imtiaz, Mushtaq, Rizwan, Arif, Yousaf, Ashraf, Shuanglian, Rizwan, Mehmood and Tu [7] in chickpea (*Cicer arietinum* L.) at V 25 mg L^{-1} application. Plants have an essential nutrient known as phosphorus (P), and its lack can cause serious damage to metabolic, biochemical, and physiological processes. Nevertheless, both V and P are chemical analogs, and it is reported that V can significantly suppress the plants' ability to absorb P. Furthermore, V causes weakness, diarrhea, nose bleeding, weight reduction, and vomiting in Humans [18]. Therefore, in plants, controlling V toxicity needs much attention for healthier plant growth and human security.

Growth regulators like cytokinin (CK), brassinosteroids (BR), salicylic acid (SA), and melatonin (MT) can be applied exogenously to combat oxidative stress by activating the plant's dual antioxidant system [8, 19, 20]. Melatonin, also known as N-acetyl-5-methoxy-tryptamine, is an organic compound having a low molecular weight and is commonly present in almost all living organisms, from animals, bacteria, and plants [21-23]. MT was first identified in 1958 in cow's pineal glands [24], however in plants, it was first discovered in 1995, later, different researchers reported its presence in different crops

such as tomatoes, rice, and pepper also observed its presence in plant different parts such leaves, roots, flowers, stems, fruits and seeds, for instance, contain about 5 to 14500 pg g^{-1} based on fresh weight [25-28]. The physiological and biochemical properties of plants are significantly influenced by MT, such as gene and enzyme regulation related to growth initiation, germination, sucrose biosynthesis, germination, and uplifting crop production [25, 29]. MT is involved in the regulation of many important processes, i.e., plant growth, flowering, circadian rhythm, fruit ripening, lateral root formation, and regeneration of root [13, 25, 29]. Moreover, MT supports the plant's total chlorophyll and carotenoid contents and revokes the chlorophyll deposition, hence increasing the photosynthesis process, and regulating the sugar and nitrogen metabolism [25, 30]. The MT also enhanced the photosynthetic capability by regulating the expression of *PsaK, PsaG, PsaO, PsaH, PsaA,* and *PsaF* genes in photo-system I, and *PsbZ, PsbP, Psb28, PsbQ, PsbY, PsbE,* and *PsbO* genes in photo-system II [31-33]. Moreover, MT is a significant anti-stress regulator and plant growth bio-stimulator, specifically under harsh environmental situations, such as ultraviolet radiation, and different stresses like heavy metals, salt, acid rain, water, cold, acid rain, drought, and heat stress [29-31, 33, 34].

This is the first-ever study about the MT defensive mechanism against V toxicity in *B. napus* in terms of plant growth and development, plant biomass, root architecture, mineral uptake, and chlorophyll contents. In order to uncover MT-upregulated genes and provide molecular insights into the mechanisms behind MT-driven tolerance, we conducted a comparative transcriptome study in addition to physiological responses. The DEGs GO/KEGG analyses, cluster analyses, WGCNA, network, and pathways analyses collectively identify the hub genes triggered by MT against V toxicity. Together, these studies improve our knowledge of how MT works to prevent V toxicity and provide important insights for creating stress-resistant *B. napus* genotypes using cutting-edge biotechnological techniques.

Materials and methods

Experimental setup and growing conditions

In the present research work, the *B. napus* genotype XiZiYuan were used from our germplasm resources at Sanya Nanfan Research Institute of Hainan University, Haikou, China. Initially, the seeds were sterilized and clean with deionized water, the seeds were then placed on wet filter paper for germination under controlled environmental conditions within a growth chamber. The gorwith conditions were maintained as: 20 °C constant temperature and 75% relative humidity (RH). After 5 days of germination, the uniform seedlings were shifted to the black hydroponic plastic pots (8.5 cm height, with 10 cm and 7 cm diameters of top and bottom, respectively) enriched with nutrient media, i.e., Hoagland Solution (HS) (pH 5.6 ± 0.1) [35]. The HS was replenished every 5 days until the seedlings reached the four-leaf stage, approximately 20 days post-transplantation, allowing for acclimation to the HS-enriched hydroponic system. Throughout this period, the growth conditions inside the growth chamber were maintained at a 16 h light/8 h dark photoperiod, RH 75%, the temperature range of 23-28 ± 1 °C, and photosynthetic photon flux density (PPFD) was maintained at 820 µmol $m^{-2}s^{-1}$.

The next step was to determine the Melatonin (MT) and Vanadium (V) optimal concentrations, as identifying effective doses was critical for assessing their impact on plant growth and development. Preliminary assays identified 100 mg L^{-1} V as the threshold causing ~50% reduction in fresh and dry weight of *B. napus*. Under this V level, MT (0–100 µmol L^{-1}) was evaluated, and 100 µmol L^{-1} was selected for its significant growth-promoting effect. All preliminary experiments were conducted under identical conditions. Seven days after transfer to half-strength Hoagland solution, seedlings were exposed to either control conditions or

100 mg L^{-1} V for 21 days. Visible stress symptoms appeared after 7 days of V exposure. Seedlings were then assigned to four treatments: control (CK), MT (100 µmol L^{-1}), V (100 mg L^{-1}), and combined treatment (MT + V; MTV). The selected V concentration was based on prior dose-response testing (25–100 mg L^{-1}), where 100 mg L^{-1} caused the greatest growth inhibition. Treatments were applied for 7 days at the four-leaf stage (20 days after transfer). MT was dissolved in ethanol and diluted with distilled water. Following treatment samples were collected separately and stored at −80°C for transcriptomic analyses.

Plant Biomass and Relative Water Content (RWC)

Plant biomass, including whole plant, root, and shoot fresh weight (FW) and dry weight (DW), was measured using three uniform seedlings per treatment. Samples were oven-dried at 105 °C for 20 min after FW determination. Root length (RL) and shoot length (SL) were recorded using a Vernier caliper. Relative water content (RWC) of leaves, roots, and shoots was calculated as:

$$Relative\ Water\ Content\ (RWC\ \%) = \frac{fw - dw}{tw - dw} \times 100$$

where TW represents turgid weight (after 24 h rehydration) [36].

Leaf Pigments, Chlorophyll Fluorescence, and Gas Exchange

Chlorophyll a (Chl a), chlorophyll b (Chl b), and carotenoids (Car) were quantified following standard protocols as described by Lichtenthaler [37]. Leaf samples were extracted in 95% ethanol with $CaCO_3$ and quartz sand, incubated in the dark for 5 min, and adjusted to 25 mL. Absorbance was recorded at 663, 645, and 470 nm for Chl a, Chl b, and Car, respectively as provided by Wellburn [38].

$$Chlorophyll\ a = 12.72\ x\ A_{663} - 2.5\ x\ A_{645}$$

$$Chlorophyll\ b = 22.91\ x\ A_{645} - 4.68\ x\ A_{663}$$

$$Carotenoids = \frac{1000\ x\ A_{470} - 3.27\ x\ Chl_a - 104.97\ x\ Chl_b}{198}$$

Chlorophyll fluorescence parameters, including minimum fluorescence (Fo), maximum fluorescence (Fm), variable fluorescence (Fv), and maximum quantum efficiency of photosystem II (Fv/Fm), were measured on fully expanded leaves using a mini-PAM fluorometer (Walz, Germany) after overnight dark adaptation as suggested by Schreiber, Schliwa and Bilger [39]. Gas exchange parameters, including net photosynthetic rate (Pn), transpiration rate (Tr), stomatal conductance (Gs), and intercellular CO_2 concentration (Ci), were measured using a LI-6400 system (LI-COR, USA) between 09:00 and 11:00 h under controlled conditions: photosynthetic photon flux density (PPFD) 800 µmol$m^{-2}s^{-1}$, CO_2 concentration 360 µmol mol^{-1}, and temperature 22 ± 1 °C.

RNA extraction, cDNA library construction, and sequencing

When plants encounter environmental stresses, they often adopt contrasting strategies to mitigate the resulting damage [40]. Increasing stress intensity, even at relatively low levels, can substantially reduce plant growth and productivity [41]. To investigate the molecular response of *B. napus* to V stress and its modulation by MT, we performed transcriptome sequencing (RNA-Seq. For this, the total RNA was extracted using the RNAprep Pure Plant Kit (TIANGEN). The extracted RNA purity and quality were checked by 1 % agarose gel electrophoresis, and a Nanodrop®spectrophotometer (Implen, CA, USA). The enzyme DNase-1 was used to remove the genomic DNA contamination, and to get the perspective amount of cDNA following the protocols of the kit (QuantiTect Reverse Transcription Kit). The RNA sequencing libraries were generated using NEBNext Ultra RNA Library Prep Kit for Illumina (NEB, USA, Catalog #: E7530L) following the manufacturer's recommendations, and index codes were added to attribute sequences to each sample. Briefly, mRNA

was purified from total RNA using poly-T oligo-attached magnetic beads. After fragmentation in NEB Next First Strand Synthesis Reaction Buffer (5X) under high temperature, the first-strand cDNA was constructed using random hexamer primer and M-MuLV Reverse Transcriptase (RNase H). Following first-strand cDNA synthesis, the second-strand cDNA was synthesised using DNA Polymerase I and RNase H. After second-strand cDNA construction, the cDNA purification and ligation to adapters were required for paired-end Illumina sequencing. The cDNA fragments of 370~420 bp in length were purified with the AMPure XP system (Beverly, USA) and were ligated to an adapter using 3 µL USER Enzyme (NEB, USA) at 37°C for 15 min, followed by 5 min at 95 °C before PCR. The PCR was performed with Universal PCR primers and Phusion High-Fidelity DNA polymerases, and the cDNA fragments were purified using the AMPure XP system. Afterward, the Agilent 5400 system （Agilent, USA） was used for library quality assessments and quantified by QPCR (1.5 nM). The qualified cDNA libraries were pooled for RNA-Seq using the Illumina NovaSeq 6000 S4 kit components in Beijing Novogene Bio-informatics Technology Co., Ltd., China.

Transcriptome analysis

The quality of the raw sequencing data was evaluated using Fastp (v0.23.1) [34] following the standard transcriptome analysis pipeline recommended by Novogene. The reference genome of *B. napus* was obtained from the *Brassica napus* multi-omics database (BnIR; http://yanglab.hzau.edu.cn/BnIR/) [35]. High-quality clean reads were aligned to the reference genome using HISAT2 (v2.0.5) [36]. Transcript assembly was performed with StringTie, and the resulting assemblies from all samples were merged using the StringTie merge function. Transcript annotation was further refined using GffCompare based on the reference genome annotation. Gene expression levels were quantified as fragments per kilobase of transcript per million mapped reads (FPKM). Raw read counts were generated using FeatureCounts, and differential expression analysis was conducted with the DESeq2 package in R. Genes with a false discovery rate (FDR) < 0.05 and an absolute log2 fold change (|log2FC|) ≥ 1 were considered significantly differentially expressed. Functional annotation of the identified genes was performed using EggNOG-mapper. Gene Ontology (GO) enrichment analysis was conducted and categorized into three major domains: biological process (BP), molecular function (MF), and cellular component (CC). Kyoto Encyclopedia of Genes and Genomes (KEGG) pathway enrichment analysis was also performed, with significantly enriched pathways identified using an adjusted *P*-value threshold of < 0.05. All graphical visualizations were generated using the ggplot2 package in R.

Weighted genes co-expression network analysis (WGCNA) and Correlation network analysis

The weighted gene co-expression network analysis (WGCNA) was performed at R (version 4.5.1) [42]. The whole genome genes with read counts were used for WGCNA analysis. Based on gene expression, the Pearson correlation coefficients were calculated. The soft threshold power was set at β=14 and the scale-free topology index customized at R^2=0.9. For module trait relationship analysis, the Pearson's correlation coefficients between the modules and traits were assessed using the 'cor' function in R4.5.1 (http://www.r-project.org/) software based on FPKM values, and a correlation graph was drawn using the ggplot2 R package (https://cran.r-project.org/web/packages/ggplot2/index.html).

Statistical analysis

The statistical analysis was performed using SPSS version 22.0 (IBM Corporation, Armonk, NY, USA), using ANOVA and LSD (least significant difference) test at the significance level of $P \leq 0.05$. The different graphs were made by different software and online tools, such as GraphPad Prism 8, Cytoscape, and SRplot (SRplot - Science and Research online plot).

Results

Effects of melatonin on vanadium-induced stress in *Brassica napus*

To comprehensively evaluate the effects of MT on V-induced stress in Brassica napus, all measured growth, water status, photosynthetic, and gas-exchange parameters were integrated into a normalized heatmap, radar plot, and percentage-change analysis (Figure 1). Compared with CK, V stress markedly reduced almost all growth, water-status, photosynthetic pigment, and gas-exchange traits in *B. napus*. Shoot length decreased from 132.6 mm in CK to 93.2 mm under V stress, while root length declined from 253.3 mm to 185.4 mm. Similarly, shoot fresh weight decreased from 2.03 g to 1.02 g, shoot dry weight from 1.23 g to 0.34 g, root fresh weight from 1.83 g to 1.12 g, and root dry weight from 0.88 g to 0.45 g, indicating severe inhibition of biomass accumulation under V toxicity (Figure 1).

Water-status parameters showed a similar declining trend. Root relative moisture content decreased from 0.034% in CK to 0.013% under V stress, shoot relative moisture content declined from 0.016% to 0.011%, and leaf relative water content was reduced from 63.31% to 30.33%. These results indicate that V stress strongly impaired plant water balance. Photosynthetic pigments and photosynthetic performance were also negatively affected by V treatment. Chlorophyll a decreased from 2.453 to 1.453 mg g^{-1} FW, chlorophyll b from 1.564 to 0.954 mg g^{-1} FW, and carotenoids from 1.784 to 1.110 mg g^{-1} FW. The SPAD index was reduced from 25.34 to 13.32, while photosynthetic assimilation declined from 21.43 to 11.12 μmol$m^{-2}s^{-1}$. Intercellular CO_2 concentration decreased from 260.23 to 143.34 μmol CO_2 mol^{-1} air, stomatal conductance from 0.21 to 0.09 mol$m^{-2}s^{-1}$, transpiration rate from 3.12 to 1.98 mmol $H_2O$$m^{-2}s^{-1}$, and Fv/Fm from 0.590 to 0.361. These reductions suggest that V stress severely disrupted photosynthetic efficiency and gas exchange (Figure 1).

In contrast, MT treatment alone improved most measured traits compared with CK. MT increased shoot length to 142.5 mm, root length to 289.7 mm, root fresh weight to 1.98 g, root dry weight to 0.99 g, root relative moisture content to 0.039%, shoot relative moisture content to 0.021%, SPAD index to 29.35, photosynthetic assimilation to 24.23 μmol m^{-2} s^{-1}, intercellular CO_2 to 271.23 μmol CO_2 mol^{-1} air, stomatal conductance to 0.25 mol m^{-2} s^{-1}, and transpiration rate to 3.55 mmol H_2O m^{-2} s^{-1} (Figure 1). These results indicate that MT promoted growth, water retention, and photosynthetic performance under non-stress conditions.

Importantly, combined MT and V treatment partially restored most traits compared with V treatment alone. Under MTV treatment, shoot length increased to 127.5 mm, root length to 222.9 mm, shoot fresh weight to 1.57 g, shoot dry weight to 0.78 g, root fresh weight to 1.67 g, and root dry weight to 0.78 g. Similarly, leaf relative water content recovered from 30.33% under V to 52.83% under MTV. Photosynthetic traits also improved under MTV compared with V, including chlorophyll a, chlorophyll b, carotenoids, SPAD index, photosynthetic assimilation, intercellular CO_2 concentration, stomatal conductance, transpiration rate, and Fv/Fm (Figure 1). Collectively, these findings suggest that melatonin mitigates vanadium-induced growth inhibition, water deficit, photosynthetic dysfunction, and physiological impairment, thereby enhancing stress tolerance in *B. napus*.

RNA-Seq and Quality Control Assessments

When plants face environmental stresses, they frequently adopt contrasting strategies to mitigate the stress effects [40]. Increased stress intensity, even at low levels, can significantly impair plant growth and productivity [41]. To investigate the mechanism of action of MT mediated defense against V-induced toxicity in *B. napus* at the molecular level by RNA-Seq. In total, ~649.35 million raw reads were generated. After filtering out low-quality reads, ambiguous bases, adaptor sequences, and sequencing artifacts, ~639.22 million clean reads were retained. The quality control assessment showed that, on average, 97.65% of bases reached Q20 and 93.72% reached Q30, with an overall 40% of GC content, confirming the high reliability of the sequencing data. The clean reads were then mapped to the *B. napus* reference genome, and

gene expression levels were quantified to obtain raw counts across all samples for downstream differential expression analysis.

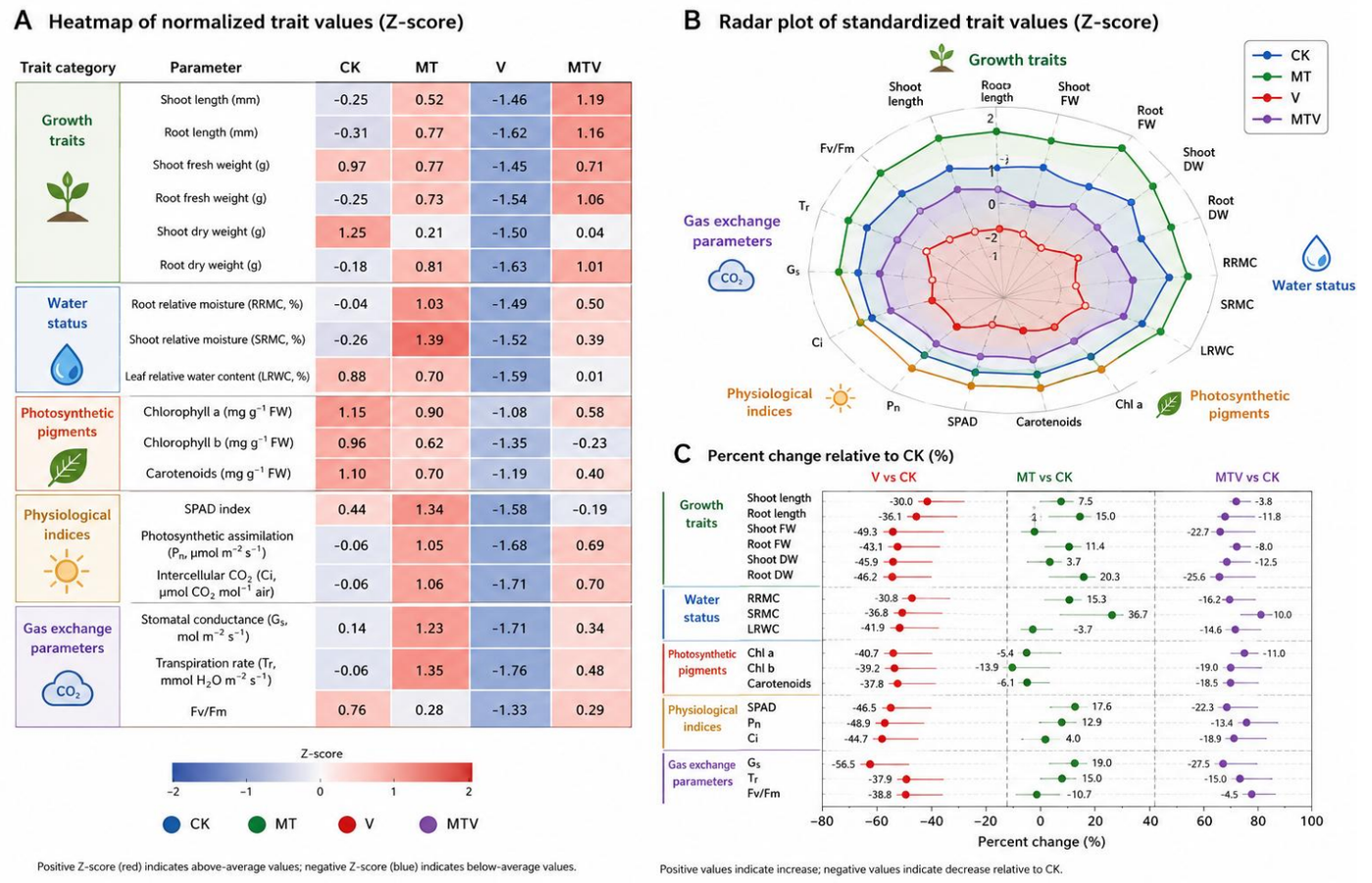


Figure 1. Integrated visualization of morphological, physiological, water status, photosynthetic pigment, and gas-exchange responses of Brassica napus under melatonin (MT) and vanadium (V) treatments. (A) Heatmap showing normalized trait values (Z-scores) across treatments. Red and blue colors indicate relatively high and low values, respectively. (B) Radar plot illustrating the overall response patterns of growth traits, water status parameters, photosynthetic pigments, physiological indices, and gas-exchange traits among treatments. (C) Percentage changes in measured parameters relative to the control (CK). CK, control; MT, melatonin treatment; V, vanadium treatment; MTV, combined melatonin and vanadium treatment. Generated with the assistance of ChatGPT (OpenAI, San Francisco, CA, USA; GPT-5.6 Sol) and subsequently edited by the authors. The authors reviewed and verified the final figure for scientific accuracy.

Analyses of Differentially expressed genes (DEGs)

To understand the transcriptional dynamics of MT-mediated responses to V stress in *B. napus,* we conducted a pairwise analysis of gene expression levels between treatments and controls. Differential expression profiling demonstrated significant transcriptional reprogramming between treatments. We obtained the highest number of DEGs in comparison CK vs. V (789 DEGs), followed by CK vs. MT (741 DEGs). Notably, CK vs. MTV exhibited a markedly reduced number of DEGs (237 DEGs), suggesting that

MT alleviated V-induced transcriptional perturbations (Figure 2A). Hierarchical clustering of DEGs clearly separated the treatments, highlighting distinct expression patterns in MT and V compared with CK, whereas MTV clustered closer to CK, indicating a restorative effect of MT under stress conditions (Figure 2B-D). To identify the MT modulating V stress-responsive genes, we performed a comparative analysis among the DEGs of CK vs MT, CK vs V, and CK vs MTV. To further explore the relationships among differentially expressed genes (DEGs) under vanadium (V) stress and melatonin (MT) treatment, an UpSet analysis was performed (Figure 2E). The results showed that CK vs MTV contained the largest number of DEGs (946), followed by CK vs MT (794) and CK vs V (789). A substantial proportion of DEGs were unique to individual comparisons, including 696 genes specific to CK vs MT, 672 genes specific to CK vs MTV, and 194 genes specific to CK vs V. Comparatively fewer genes were shared among the treatment groups, with 57 genes commonly differentially expressed between CK vs MTV and CK vs MT, 31 genes shared between CK vs MTV and CK vs V, and 7 genes shared between CK vs MT and CK vs V. Notably, only 5 genes were commonly differentially expressed across all three comparisons (Figure 2E). These findings indicate that MT treatment, V stress, and their combined effects induce largely distinct transcriptional responses, while only a limited set of genes may participate in a common regulatory network underlying stress adaptation and melatonin-mediated protection.

Functional Enrichment Analysis of DEGs

To identify the functional annotation of DEGs in *B. napus,* we performed GO enrichment analysis of up- and down-regulated DEGs among CK vs MT, CK vs V, and CK vs MTV treatments, which can categorize the heavy metal stress-related genes associated with key biological processes. Figure 3 showed the top 10 significant stress-related GO terms based on (*adjusted P ≤0.05*). In CK vs MT treatment, 247 up-regulated DEGs were mainly involved in protein complex oligomerization (GO:0051259), auxin bio-synthetic process (GO:0009851), wax bio-synthetic and metabolic processes (GO:0010025, GO:0010166), protein self-association & unfolded protein binding (GO:0043621, GO:0051082), hydrolase and oxidoreductase activities (GO:0016815, GO:0016661), and carbohydrate trans-membrane transporter activity (GO:0015144) (Figure 3A). In comparison, most of 494 down-regulated genes were associated with tropism and phototropism (GO:0009606, GO:0009638), regulation of reactive oxygen species bio-synthetic process (GO:1903426), tetraterpenoid metabolic process (GO:0016108), production of lsiRNA and ta-siRNAs involved in RNA interference (GO:0010599; GO:0010267), gene silencing by miRNA (GO:0035195), and carotenoids catabolic and metabolic processes (GO:0016118, GO:0016108) (Figure 3C).

In CK vs V treatment majority of 361 up-regulated DEGs were involved in regulation of meristem growth (GO:0010075), plant-type secondary cell wall bio-genesis (GO:0009834), meristem growth (GO:0035266), pectinesterase inhibitor activity and pectinesterase activity (GO:0046910, GO:0030599), inorganic anion trans-membrane transporter activity (GO:0015103), solute: cation symporter activity (GO:0015294), and integral component of plasma membrane activity (GO:0005887), in contrast the 428 down-regulated genes were mostly associated with protein refolding (GO:0042026), purine nucleoside triphosphate metabolic process (GO:0009144), cellular response to phosphate starvation (GO:0016036), chaperone-mediated protein folding (GO:0061077), ribonucleoside and nucleoside monophosphate metabolic process (GO:0009161, GO:0009141), ATP metabolic process (GO:0046034), heat shock protein binding (GO:0031072), and unfolded protein binding (GO:0051082). In CK vs MTV 157 up-regulated DEGs were associated with jasmonic acid metabolic process (GO:0009694), and phenylpropanoid metabolic process (GO:0009698), in comparison, most of the 80 down-regulated DEGs in CK vs MTV treatment were involved in hydrogen peroxide transmembrane transport (GO:0080170),

protein refolding (GO:0042026), cellular response to unfolded protein (GO:0034620), cellular response to nitrogen starvation (GO:0006995), misfolded protein binding (GO:0051787), channel activity (GO:0015267), passive transmembrane transporter activity (GO:0022803), plastoglobule (GO:0010287), central vacuole and storage vacuole (GO:0042807, GO:0000322), and protein storage vacuole activity (GO:0000326).

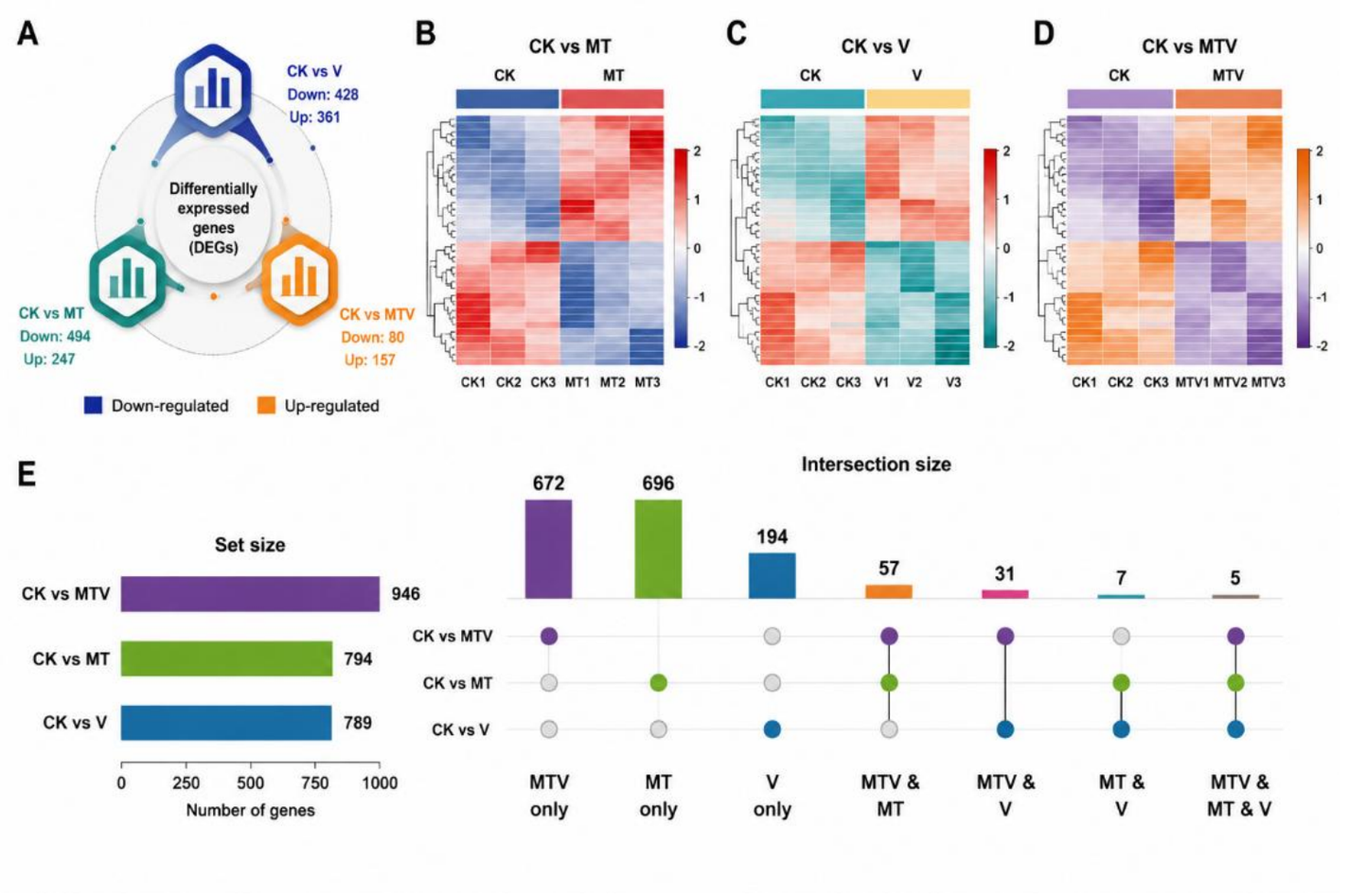


Figure 2. Comparative analyses of differentially expressed genes (DEGs) in *B. napus* seedlings under different treatments and control: (A) Total number of upregulated and downregulated DEGs in all treatments, (B-D) Clustering heat-map of DEGs; CK vs MT, CK vs V, and CK vs MTV, respectively, (E) UpSet plot showing the distribution and overlap of DEGs among the three pairwise comparisons (CK vs V, CK vs MT, and CK vs MTV). Horizontal bars on the left indicate the total number of DEGs identified in each comparison (set size), while vertical bars represent the number of unique and shared DEGs among comparisons (intersection size). Filled circles connected by lines indicate the specific comparisons contributing to each intersection. The analysis revealed that most DEGs were comparison-specific, whereas only a small number of genes were shared among multiple comparisons, suggesting distinct transcriptional responses to vanadium stress, melatonin treatment, and their combined effects. Generated with the assistance of ChatGPT (OpenAI, San Francisco, CA, USA; GPT-5.6 Sol) and subsequently edited by the authors. The authors reviewed and verified the final figure for scientific accuracy.

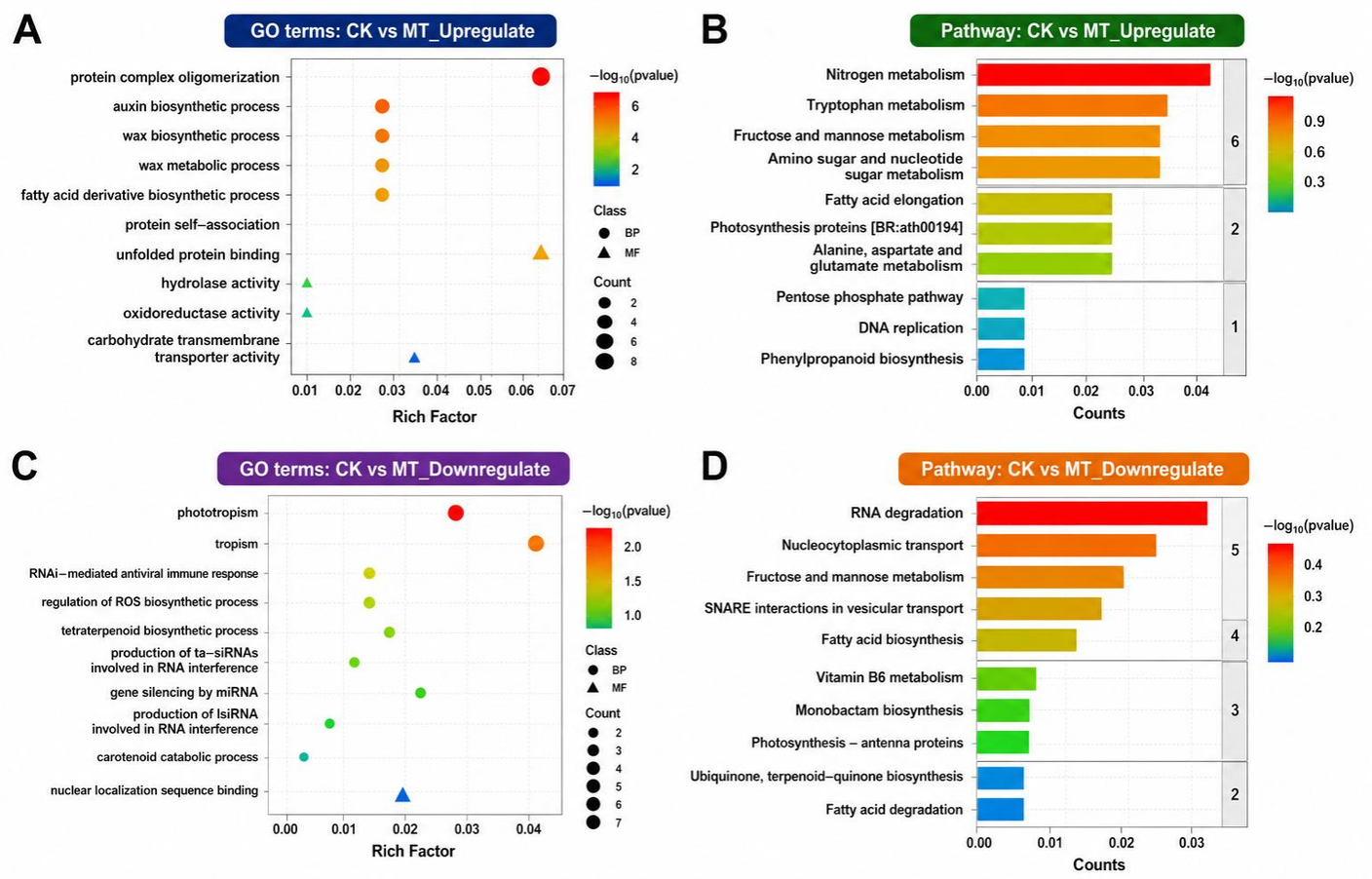


Figure 3. The Gene Ontology (GO) and Kyoto Encyclopedia of Genes and Genomes (KEGG) annotation and enrichment analysis of up- and down-regulated DEGs in melatonin (MT) treatment, as compared to control (CK). (A) GO enrichment analysis of up-regulated DEGs. (B) KEGG enrichment analysis of up-regulated DEGs. (C) GO enrichment analysis of down-regulated DEGs, and (D) KEGG enrichment analysis of down-regulated DEGs. The x-axis represents the enrichment factor and gene counts, and the y-axis represents GO/KEGG terms. The size of circular dots and bars shows the number of DEGs in each term and pathway, respectively. The color gradient from green (min.) to red (max.) shows the significance of each term and pathway based on the *p*-value of the DEGs.

To identify the significant pathways in *B. napus* associated with V stress responses, we used the KEGG database to identify the key genes in CK vs MT, CK vs V, and CK vs MTV treatments involved in KEGG pathways. In CK vs MT the 741 up- and down-regulated DEGs enriched in 107 KEGG pathways including, nitrogen metabolism (ath00910), tryptophan metabolism (ath00380), photosynthesis proteins and photosynthesis-antenna proteins (ath00194, ath00196), fructose and mannose metabolism (ath00051), fatty acid elongation (ath00062), pentose phosphate pathway (ath00030), DNA replication (ath03030), and phenylpropanoid biosynthesis (ath00940), ubiquinone and other terpenoid-quinone biosynthesis (ath00130), RNA degradation (ath03018), and fatty acid degradation (ath00071) (Figure 3B and 3D). The 789 up- and down-regulated DEGs in CK vs V treatment enriched in 61 KEGG pathways including,

photosynthesis-antenna proteins (ath00194), steroid biosynthesis (ath00100), nucleotide excision repair (ath03420), glycolysis/gluconeogenesis (ath00010), galactose metabolism (ath00052), amino sugar and nucleotide sugar metabolism (ath00520), sulfur metabolism (ath00920), and RNA degradation (ath03018). The 237 up- and down-regulated DEGs in CK vs MTV enriched in 20 KEGG pathways including cytochrome P450 (ath00199), proteasome (ath03050), photosynthesis and photosynthesis proteins (ath00195, ath00194), ubiquinone and other terpenoid-quinone biosynthesis (ath00130), porphyrin metabolism (ath00860), photosynthesis-antenna proteins (ath00196), phenylpropanoid biosynthesis (ath00940), and RNA degradation (ath03018).

Overall, KEGG enrichment analysis revealed distinct as well as overlapping metabolic and regulatory pathways among the three comparisons. CK vs MT showed the broadest metabolic reprogramming, with 741 DEGs enriched across 107 diverse pathways, highlighting enhanced primary metabolism (nitrogen, tryptophan, carbohydrate, fatty acid) and photosynthetic processes, alongside stress-related phenylpropanoid biosynthesis. CK vs V displayed a narrower but stress-specific enrichment profile, with 789 DEGs in 61 pathways, predominantly affecting photosynthesis, lipid and sugar metabolism, DNA repair, and sulfur metabolism, indicating V-induced disruption of both energy production and repair mechanisms. In contrast, CK vs MTV exhibited the smallest DEG set (417 DEGs) and enrichment in only 20 pathways, largely overlapping with photosynthesis, phenylpropanoid biosynthesis, ubiquinone biosynthesis, and proteasome activity, suggesting that MT treatment under V stress partially restored metabolic balance while maintaining activation of key detoxification and defense pathways.

Cluster analysis of DEGs and their Functional Annotation

We used FPKM expression values of 1767 DEGs (**Figure** 4) to perform hierarchical clustering to evaluate expression patterns of DEGs among all treatments: CK, MT, V, and MTV in *B. napus*. The *hclust* method was used to identify the clusters with similar patterns of expression change. As a result, we obtained six clusters (Clusters C1-C6), among which two clusters, cluster C2 and cluster C6, were significantly associated with MTV and MT, respectively (Figures 4A). Notably, cluster C2 contained 218 highly expressed DEGs associated with MT in combined treatment with V, while the expression of these genes was down-regulated in V separate treatment. A total of 230 DEGs were found in cluster C6, which were significantly up-regulated by MT single treatment as a growth enhancer; in contrast, these genes were down-regulated by V stress (Figure 4A).

Next, we explored the biological functions of these two clusters of DEGs by performing GO and KEGG enrichment analysis (Figures 4B-E). The 218 DEGs of MTV associated cluster C2 were primarily enriched in hydrolase and jasmonic acid hydrolase activity (GO:0016810, GO:0120091), oxidoreductase activity (GO:0016639), phenylalanine ammonia-lyase activity (GO:0045548), actin filament binding (GO:0051015), jasmonic acid metabolic process (GO:0009694), regulation of cell death (GO:0010941), regulation of phenylpropanoid metabolic processes (GO:2000762, GO:0009698), and regulation of jasmonic acid mediated signaling pathways (GO:2000022) (Figure 4B). The KEGG pathways analysis revealed that these DEGs were mainly associated with nitrogen metabolism (ath00910), GTP-binding proteins (ath04031), phenylpropanoid biosynthesis (ath00940), cytochrome P450 (ath00199), flavonoid biosynthesis (ath00941), phenylalanine metabolism (ath00360), arginine biosynthesis (ath00220), and tryptophan, glycerophospholipid, cysteine and methionine metabolism (ath00380, ath00564, ath00270) (Figure 4D).

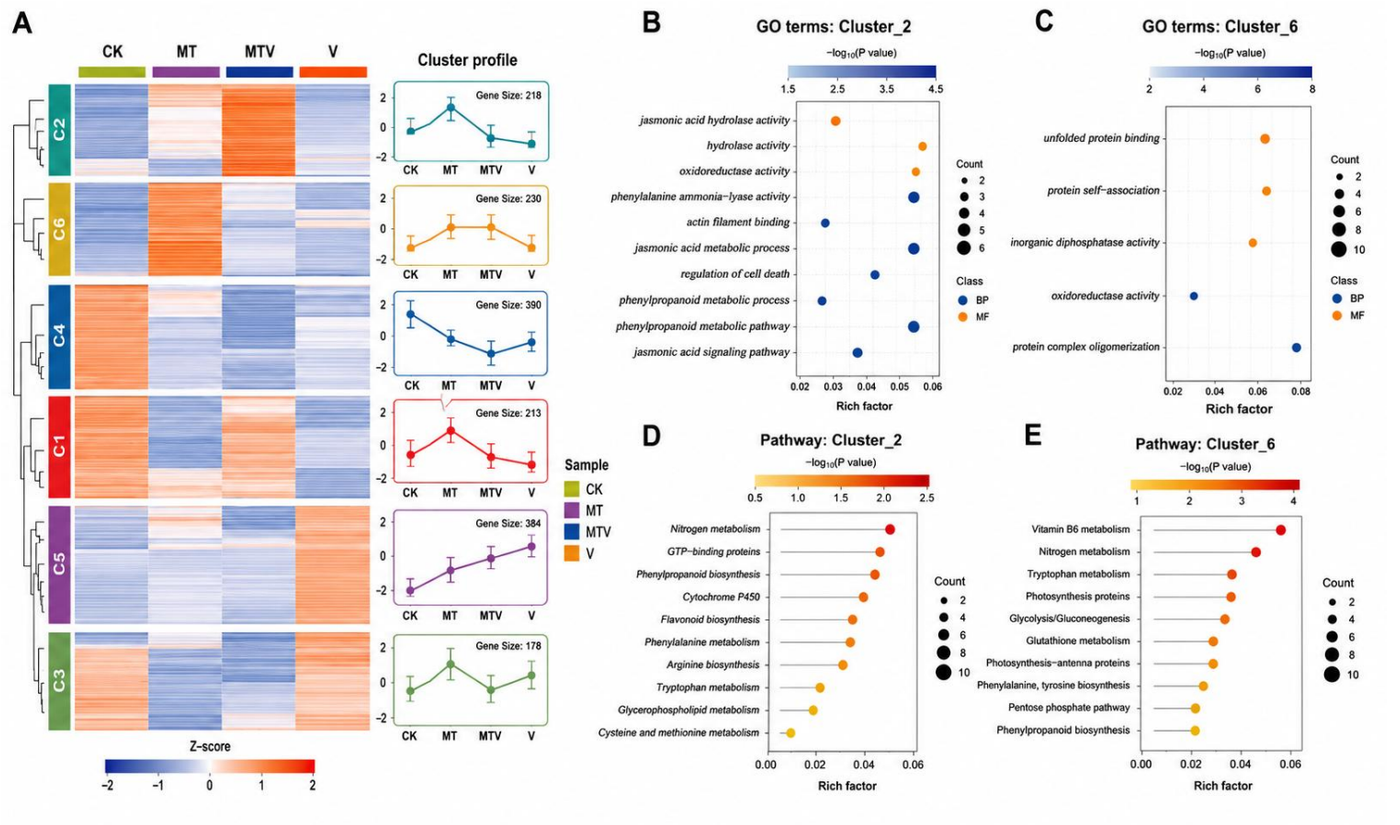


Figure 4. The clustering of expression patterns of DEGs and GO/KEGG enrichment analysis of MTV- and MT-associated clusters; C2 and C6 genes, respectively, (A) Hierarchical clustering of DEGs showing six distinct expression clusters (C1–C6); clusters C2 and C6 were significantly associated with MTV and MT treatments, respectively, red line in small box of each cluster represents the mean changes in DEGs expression pattern among each treatment. (B) GO enrichment analysis of MTV-associated DEGs in cluster C2. (C) GO enrichment analysis of MT-associated DEGs in cluster C6. (D) KEGG pathway enrichment of MTV-associated DEGs in cluster C2. (E) KEGG pathway enrichment of MT-associated DEGs in cluster C6. The x-axis represents the enrichment factor and gene counts, and the y-axis represents the cluster number and GO/KEGG terms. The size of circular dots and bars shows the number of DEGs in each term and pathway, respectively. The color gradient from green (min.) to red (max.) shows the significance of each term and pathway based on the p-value of the DEGs.

The 230 DEGs of MT-associated cluster C6 were predominantly enriched in unfolded protein binding (GO:0051082), protein self-association (GO:0043621), inorganic diphosphatase activity (GO:0004427), oxidoreductase activity, acting on other nitrogenous compounds as donors (GO:0016661), and protein complex oligomerization (GO:0051259) (Figure 4C), while mainly associated with following KEGG pathways; vitamin B6 metabolism (ath00750), nitrogen metabolism (ath00910), tryptophan metabolism (ath00380), photosynthesis and photosynthesis-antenna proteins (ath00194, ath00196), phenylalanine, tyrosine and tryptophan biosynthesis (ath00400), and phenylpropanoid biosynthesis (ath00940) (Figure 4E). Collectively, these results indicate that MT application modulates key metabolic and signaling pathways-particularly those related to jasmonic acid metabolism, phenylpropanoid biosynthesis, and protein-folding processes-which may enhance defense responses and facilitate metabolic reprogramming in *B. napus* under V-induced stress.

Weighted Gene Correlation Network Analysis (WGCNA) and module trait relationship

In the current study, we used FPKM values of whole genome genes with read counts to perform a WGCNA analysis to identify the key modules and significant intramodular hub genes associated with measured phenotypic traits and stress parameters among all treatments: CK, MT, V, and MTV in *B. napus* (Figure 5). The soft threshold power was set at β=14 and the scale-free topology index customized at R^2=0.9 (Figure 5A). The hierarchical clustering dendrogram represents the similar expression modules of eigengene groups based on their correlations. The red horizontal line marks the cut-off threshold for merging similar modules, and modules below this line were merged to minimize the redundancy level while preserving biologically significant clusters (Figure 5B). As a result, the genes were clustered and primarily divided into 24 expression modules; however, after merging (merge cut height=0.25) to minimize the plethora and to get significant modules, we finally got 17 stable expression modules (Figure 5B, C).

The module-trait relationship was measured by applying the Pearson correlation coefficient (PCC), for which the criteria were set as a PCC (r = 0.5) and significance of *p*-value ($p \leq 0.05$). The range of gene numbers among these modules was from 68 to 735 genes. Among these 17 modules, two modules, black and tan, were significantly connected with phenotypic traits and stress-related parameters. The tan module 133 genes were significantly correlated with SL, RL, plant biomass, RFW, RDW, and RRWC phenotypic traits, and Pn, Ci, Gs, Tr, SPAD stress parameters (Figure 5D). The 613 genes of the black module were significantly correlated with leaf length and maximum fluorescence of PSII, Fv/Fm, which are highly correlated with each other (Figure 5D).

Network Construction, Identification of Hub Genes, and GO/KEGG enrichment analysis of black and tan modules

To pinpoint key stress-responsive genes in *B. napus,* we conducted a network analysis of the black and tan modules, and the top 25 genes from each module were taken as the candidate hub genes for module-specific network construction (Figure 6A and 6B). Among the hub genes, twelve genes in black module were identified, including *BnA06g0250300.1* encodes Cox19-like CHCH family protein; *BnA10g0414710.1* encodes a plasma membrane localized LITAF domain protein, *BnA04g0163440.1* encodes 60S ribosomal protein L35a-1 (*RPL35AA*, *A. thaliana*); *BnA07g0294190.1* encodes ACD11 homolog protein (*At4g39670, A. thaliana*); *BnC04g0649390.1* encodes eukaryotic translation initiation factor 5A-2 (*ELF5A-2*, *A. thaliana*), *BnA04g0169260.1* encodes glutaredoxin-C2 (*GRXC2*, *A. thaliana*); *BnA09g0384230.1* encodes hydrophobic protein RCI2A (*RCI2A*, *A. thaliana*); *BnC08g0880780.1* encodes photosynthetic NDH subunit of lumenal location 2, chloroplastic, (*PNSL2*, *A. thaliana*); *BnC05g0731050.1* encodes protein-tyrosine-phosphatase MKP1 (*MKP1*, *A. thaliana*); *BnA09g0356920.1* encodes thioredoxin H-type, (thioredoxin H-type, *Brassica campestris*); *BnA06g0252650.1* encodes trans-cinnamate 4-monooxygenase (*CYP73A5*, *A. thaliana*) and *BnC01g0428770.1* encodes V-type proton ATPase subunit c5 (*VHA-c5*, *A. thaliana*). Three genes were identified in the tan module, including, *BnC07g0822390.1* encodes 5'-adenylylsulfate reductase 3, chloroplastic (*APR3*, *A. thaliana*); *BnC07g0809180.1,* which encodes peptidyl-prolyl cis-trans isomerase FKBP65 (*FKBP65*, *A. thaliana*); and *BnC05g0700640.1,* which encodes phosphatidylinositol-glycan biosynthesis class F protein (*Mus musculus*) (Figure 6A and 6B).

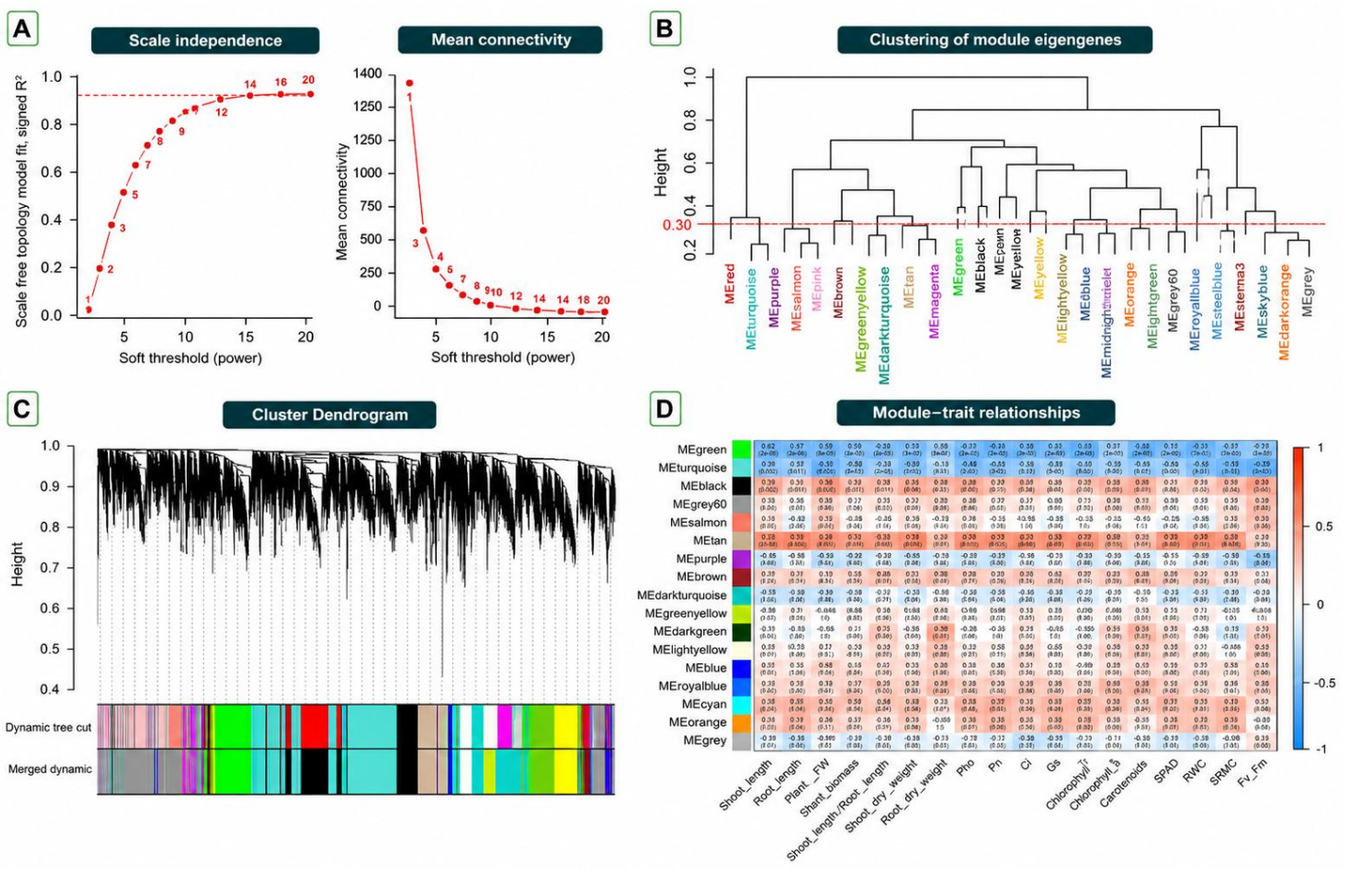


Figure 5. Weighted Gene Correlation Network Analysis (WGCNA) of whole genome genes with read counts, (A) Determination of soft-threshold power for network construction based on scale-free topology criterion (left) and mean connectivity (right). The soft threshold power was set at β=14 and the scale-free topology index customized at R^2=0.9. (B) Hierarchical clustering dendrogram of module eigengenes showing correlations among modules, with the red line indicating a threshold for merging similar modules. (C) Gene dendrogram based on topological overlap, with modules identified by dynamic tree cut and merged dynamic colors displayed below. (D) Heatmap of module-trait relationships showing Pearson correlation coefficients (r = 0.5) and significance of p-value ($p \leq 0.05$) between module eigengenes and various phenotypic traits. Color scale denotes correlation strength from -1 (blue) to 1 (red).

To identify the process and pathways associated with black and tan module genes, we performed GO and KEGG enrichment analysis. The 746 genes of black and tan module, enriched in BP, including protein complex oligomerization (GO:0051259), negative regulation of plant-type hypersensitive response (GO:0034051), programmed cell death induced by symbiont (GO:0034050), regulation of cellular stress response (GO:0080135), and negative regulation of programmed cell death (GO:0043069), while in MF, including unfolded protein binding (GO:0051082), protein self-association (GO:0043621), oxidoreductase activity, acting on a sulfur group of donors (GO:0016667), MAP kinase phosphatase activity (GO:0033549), and glutathione-disulfide reductase (NADPH) activity (GO:0004362). The KEGG analysis showed the enrichment in stilbenoid, diarylheptanoid and gingerol biosynthesis (ath00945), glycosylphosphatidylinositol (GPI)-anchor biosynthesis (ath00563), Flavonoid biosynthesis

(ath00941), sulfur metabolism (ath00920), ubiquinone and other terpenoid-quinone biosynthesis (ath00130), photosynthesis (ath00195), photosynthesis proteins (ath00194), proteasome (ath03051), cytochrome P450 (ath00199), and phenylpropanoid biosynthesis (ath00940) (Figure 6C and 6D). Collectively, these findings position the black and tan modules as molecular hubs linking lipid- and redox-mediated signaling to metabolic reprogramming, underpinning adaptive stress responses in *B. napus*.

Discussion

Heavy metal stress has emerged as a key limitation on global agriculture, with V contamination widely seen as a serious threat to agricultural productivity and food security [12]. The present research work represents the first comprehensive, transcriptome-wide exploration of MT mediated defense mechanisms against V stress in *B. napus*. Based on RNA-seq, WGCNA, and pathway enrichment analysis, we demonstrate that exogenous MT significantly restores growth, reprograms stress-responsive pathways under V toxicity. These findings not only strengthen the established role of MT in alleviating abiotic stresses but also extend its functional spectrum to the less-studied V toxicity in *B. napus*, offering novel mechanistic insights and translational potential for developing V-resilient *B. napus* cultivars. Plants can naturally scavenge ROS damage due to heavy metals by improving antioxidant machinery; however, if this system becomes weak, then supplementation of some exogenous compounds having signification antioxidant-system supporting abilities can improve the plants' defence against these stresses [21]. MT is one of such exogenous compounds having significant antioxidant properties, and supports the plant immunity, uplifts the stress resistance, acts as a signaling molecule, and upregulates the stress-resistant genes and level of endogenous MT under a stressful environment [24]. Moreover, different recent research publications suggest that MT plays a prominent protective role against abiotic stresses in different plants such as kiwifruit [43], rubber tree [44], and tomato [32].

Heavy metal toxicity leads to a reduction in photosynthetic activity, directly damages the system [45], lowers the CO_2 exchange [20, 46], and can cause stomatal closure [47, 48]. Plant growth is positively correlated with photosynthetic activity; a higher photosynthesis rate corresponds to improved plant growth and vice versa. Photosynthesis is directly correlated with chlorophyll and carotenoid accumulation [49]. The high accumulation of V in *B. napus* significantly decreased chl a, chl b, carotenoid, and SPAD index, Pn, intercellular CO_2 concentration, Gs, Tr, maximum quantum of PSII, and Fv/Fm levels in the present investigation. Notably, ME supplementation significantly improved the content of these photosynthetic pigments and parameters in *B. napus* seedlings (Figure 1). Our results are consistent with findings in various crops, including rice, mustard, and chickpea [6, 7, 12, 50], where V accumulation decreased and MT significantly increased the photosynthetic pigments and parameters. The results revealed that MT effectively mitigated V toxicity by supporting the photosynthetic machinery, thereby enhancing *B. napus* seedling growth (Figure 1). This is consistent with the physiological observations of increased Fv/Fm ratio (Figure 1) and inhibited chlorophyll degradation, suggesting that MT maintains photosynthetic efficiency by regulating the expression of photosynthesis system genes.

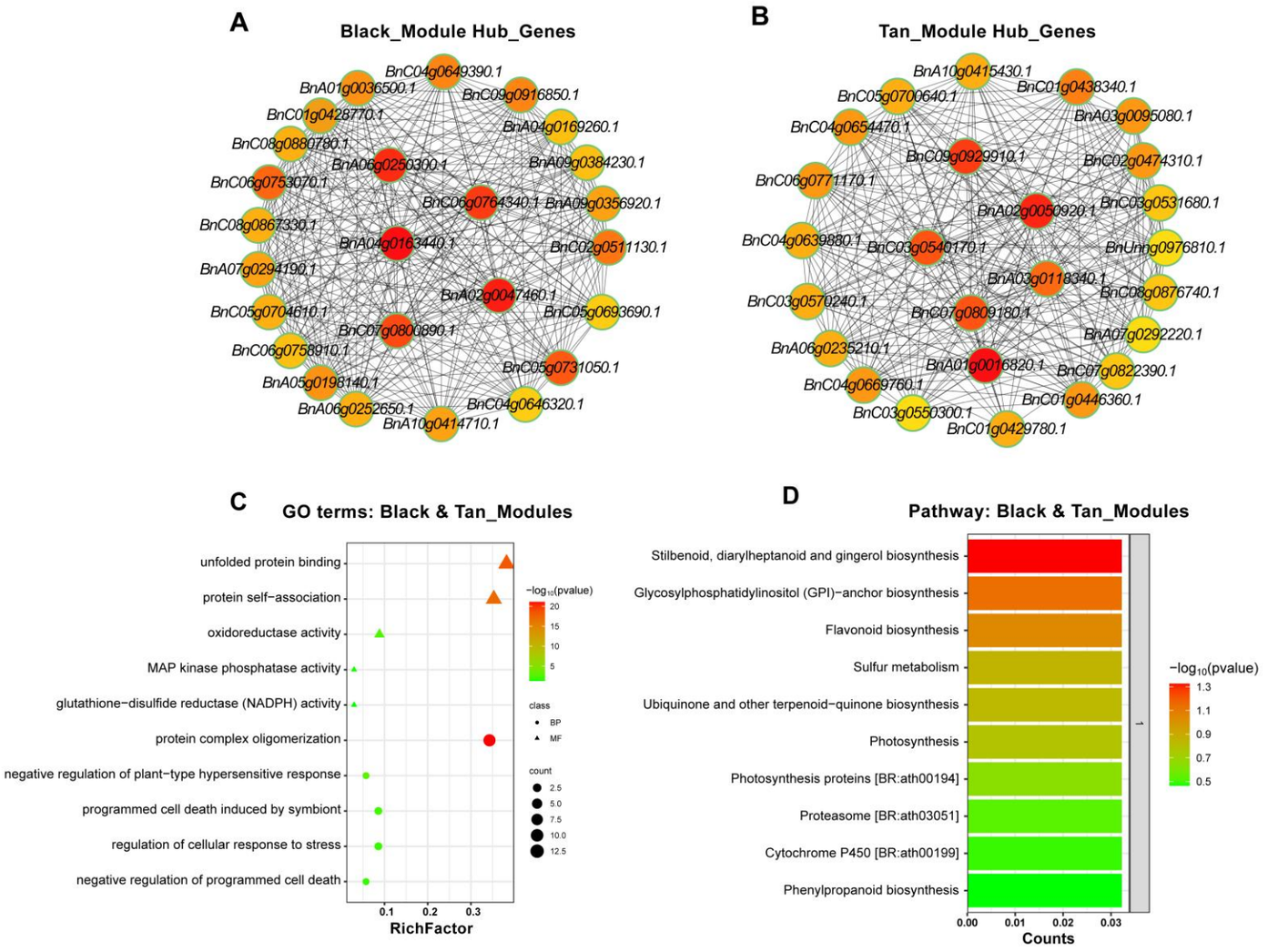


Figure 6. Hub gene networks and functional enrichment of stress-responsive modules in *B. napus*. (A, B) Co-expression networks of the top 25 candidate genes from the black (A) and tan (B) modules identified by weighted gene co-expression network analysis (WGCNA). Node size represents intramodular connectivity, and node color scales from yellow (lower connectivity) to red (higher connectivity). Edges indicate significant co-expression correlations. (C) Gene Ontology (GO) enrichment analysis of the black and tan modules showing significantly enriched biological processes (BP), molecular functions (MF), and cellular components (CC). Dot size represents the number of genes in each term, and color indicates statistical significance ($-\log_{10}$ *p*-value). (D) KEGG pathway enrichment analysis of the black and tan modules. Bar length reflects the number of genes annotated in each pathway, and color represents enrichment significance ($-\log_{10}$ *p*-value).

RNA-seq revealed that V stress caused extensive transcriptional perturbations, while MT reduced DEG numbers and restored expression patterns closer to CK (Figures 2). Similar restorative transcriptomic effects of MT have been observed in *tomato* under drought [51, 52], in rice under Al toxicity [53, 54], and in *Arabidopsis* under salinity [55]. Using RNA-seq, we identified ~639.22 million clean reads. We compare the expression data of leaves in MT, V, and MTV with CK, and identify 794, 789, and 946 DEGs in CK vs. MT, CK vs. V, and CK vs. MTV, respectively

(Figures 2). Further these DEGs were involved in protein complex oligomerization, auxin bio-synthetic process, protein self-association & unfolded protein binding, hydrolase and oxidoreductase activities, tropism and phototropism, regulation of reactive oxygen species bio-synthetic process, production of lsiRNA and ta-siRNAs involved in RNA interference, gene silencing by miRNA, hydrogen peroxide transmembrane transport, protein refolding, protein storage vacuole activity, carotenoids catabolic and metabolic processes, ribonucleoside and nucleoside monophosphate metabolic process, ATP metabolic process, heat shock protein binding, jasmonic acid metabolic process and phenylpropanoid metabolic process, that are align with the results of [56, 57].

Our clustering analysis classified all the DEGs into six clusters, where two clusters, C6 and C2, contain genes that were triggered by MT alone or under V stress. Together, these clusters contain a total of 248 hub genes, in which the MT-specific (C6) cluster has 230 genes, and the MTV-specific (C2) cluster has 218 genes. The gene ontology revealed that these genes were mostly involved in redox regulation, protein complex oligomerization, protein folding, phenylpropanoid metabolic processes, hormone metabolism, and jasmonic acid signaling, suggesting that MT coordinates hormonal crosstalk with stress defenses (Figures 4). These results complement previous findings where MT modulated auxin, ABA, and JA pathways to fine-tune stress responses [29-31, 58].

The WGCNA analyses classified all the genes into 17 stable expression modules based on FPKM values, among them two modules, black and tan, containing 613- and 133-genes, respectively, significantly correlated with SL, RL, plant biomass, RFW, RDW, and RRWC phenotypic traits, and Pn, Ci, Gs, Tr, SPAD stress parameters, leaf length, and maximum fluorescence of PSII, Fv/Fm (Figure 5B and 5D). These genes are known to participate in glutathione metabolism, peroxidase activity, and cytochrome P450-mediated detoxification, respectively, all of which are critical for heavy metal tolerance. The ability of MT to activate such key hubs confirms its status as a master regulator of stress resilience. The top 25 genes from each module were taken as the candidate hub genes for module-specific network construction (Figure 5A and 5B). Among these twelve genes in black module and three genes from tan module were selected as hub genes that were involved in encoding a plasma membrane localized LITAF domain protein, 60S ribosomal protein, encodes eukaryotic translation initiation factor 5A-2, glutaredoxin-C2, hydrophobic protein RCI2A, encodes photosynthetic NDH subunit of lumenal location 2, chloroplastic, protein-tyrosine-phosphatase MKP1, 5'-adenylylsulfate reductase 3, and peptidyl-prolyl cis-trans isomerase FKBP65 (Figure 5C and 5D). Similar hub genes were reported in *Arabidopsis* and *peanut* under Cd and Pb stresses [55, 59], suggesting conserved molecular pathways across species. Most importantly, these modules identify potential genetic targets for future rapeseed breeding and biotechnological interventions.

Taken together, our findings demonstrate that MT reduces V toxicity in *B. napus* by employing a multi-layered defense strategy that includes: restricting metal uptake, restoring photosynthetic efficiency, reducing oxidative stress, stimulating antioxidant enzymes, and reprogramming transcriptomic networks, particularly those governing phenylpropanoid metabolism and redox regulation. While previous research works have demonstrated MT's roles under Cd, Ni, and Al stresses [5, 60, 61], our findings provide the first transcriptomic evidence of MT's role in mitigating V toxicity. This broadens the scope of MT research to include a new class of heavy metal contaminants and underscores its potential as a bio-regulator for sustainable rapeseed production on contaminated soils.

Conclusion

Heavy metal toxicity, particularly vanadium (V), is a growing threat to sustainable agriculture and global

food security. This study represents transcriptomic evidence that melatonin (MT) significantly mitigates V toxicity in *Brassica napus*. Transcriptome-wide reprogramming at the molecular level showed that MT reduced excessive DEG fluctuations brought on by V stress, bringing expression patterns closer to the control. Cluster analyses (C2, C6) show MT-specific activation of genes involved in phenylpropanoid biosynthesis, jasmonic acid metabolism, and protein folding. Weighted gene co-expression network analysis (WGCNA) identified the black and tan modules as strongly correlated with photosynthesis, biomass, and stress traits, pinpointing hub genes *NAC072, MYB122, WRKY33, PER72, GSTU19, CYP82G1, ELF5A-2, Cox19-like, RCI2A, GRXC2, MKP1, PNSL2, CYP73A5, thioredoxin H-type, FKBP65, APR3, VHA-c5,* and *PIG-F* as central regulators of stress tolerance. These hub genes converge on redox regulation, secondary metabolism, detoxification, and hormone signaling emerging as an essential pathway. Collectively, our findings show that MT coordinates a multi-layered defensive strategy against V toxicity, which includes limiting harmful ion intake, strengthening photosynthetic and antioxidative machinery, and altering transcriptional networks and metabolic pathways. The discovery of hub genes presents valuable opportunities for genetic engineering and precision breeding, while integrative physiological evidence supports MT use as a viable agronomic intervention. This study shows MT not only as a master regulator of abiotic stress tolerance in rapeseed but also as a scalable strategy for maintaining crop yield on heavy metal-contaminated soils, providing both fundamental insights and translational potential for sustainable agriculture.

Data availability

The datasets generated and/or analyzed during the current study are available in the NCBI SRA repository, PRJNA1370522, https://www.ncbi.nlm.nih.gov/bioproject/PRJNA1370522

Acknowledgments

Not applicable

Conflict of interest

The authors declare that they have no conflict of interest.

Author Contribution

The authors confirm their contributions to the paper as follows: LUK: Conceptualization, methodology, investigation and experimental work, formal analysis and validation, writing—original draft preparation, and writing—review and editing. EM: Seedling management and stress treatments. WS: Formal analysis and validation, and writing—review and editing. ZC: Formal analysis and validation, and writing—review and editing. MI: Formal analysis and validation. MU: Formal analysis and validation, and writing—review and editing. YL: Writing—review and editing. All authors have read and approved the final version of the manuscript and agree to be accountable for their contributions to the work.

Funding

Not applicable

Ethics Statement

Not applicable

Publisher's note

The views expressed in this article are solely those of the authors and do not necessarily reflect those of their institutions, the publisher, editors, or reviewers. Any product mentioned is neither guaranteed nor endorsed by the publisher.

Generative AI Statement

During the preparation of this manuscript, the authors used ChatGPT (OpenAI, GPT-5.6 Sol) to assist with the generation of scientific illustrations based on author-provided concepts and scientific information. The authors reviewed, edited, and verified the generated outputs and take full

responsibility for the accuracy, validity, and integrity of the figures and the content of this publication.

Dates

Received 08 July 2026; Revised 14 October 2026; Accepted 31 October 2026; Published online 04 November 2026

References

[1] H.-Z. Wang, New-demand oriented oilseed rape industry developing strategy, *Chinese Journal of Oil Crop Sciences,* vol. 40, no. 5, pp. 613-617, 2018.

[2] W. Ahmed, Y. Xia, R. Li, G. Bai, K. H. Siddique, and P. Guo, Non-coding RNAs: Functional roles in the regulation of stress response in Brassica crops, *Genomics,* vol. 112, no. 2, pp. 1419-1424, 2020.

[3] V. Chinnusamy, K. Schumaker, and J. K. Zhu, Molecular genetic perspectives on cross-talk and specificity in abiotic stress signalling in plants, *Journal of experimental botany,* vol. 55, no. 395, pp. 225-236, 2004.

[4] Q. U. Zaman, V. Garg, A. Raza, M. F. Nazir, L. Hui, D. Khan, A. A. Khokhar, M. A. Hussain, H. F. Wang, and R. K. Varshney, Unique regulatory network of dragon fruit simultaneously mitigates the effect of vanadium pollutant and environmental factors, *Physiologia plantarum,* vol. 176, no. 4, p. e14416, 2024.

[5] M. A. Altaf, R. Shahid, M.-X. Ren, M. M. Altaf, M. S. Jahan, and L. U. Khan, Melatonin mitigates nickel toxicity by improving nutrient uptake fluxes, root architecture system, photosynthesis, and antioxidant potential in tomato seedling, *Journal of Soil Science and Plant Nutrition,* vol. 21, no. 3, pp. 1842-1855, 2021.

[6] M. Imtiaz, M. A. Mushtaq, M. A. Nawaz, M. Ashraf, M. S. Rizwan, S. Mehmood, O. Aziz, M. Rizwan, M. S. Virk, and Q. Shakeel, Physiological and anthocyanin biosynthesis genes response induced by vanadium stress in mustard genotypes with distinct photosynthetic activity, *Environmental Toxicology and Pharmacology,* vol. 62, pp. 20-29, 2018.

[7] M. Imtiaz, M. A. Mushtaq, M. S. Rizwan, M. S. Arif, B. Yousaf, M. Ashraf, X. Shuanglian, M. Rizwan, S. Mehmood, and S. Tu, Comparison of antioxidant enzyme activities and DNA damage in chickpea (Cicer arietinum L.) genotypes exposed to vanadium, *Environmental Science and Pollution Research,* vol. 23, no. 19, pp. 19787-19796, 2016.

[8] S. K. Bose and P. Howlader, Melatonin plays multifunctional role in horticultural crops against environmental stresses: A review, *Environmental and experimental botany,* vol. 176, p. 104063, 2020.

[9] L. Chen, Y.-y. Zhu, H.-q. Luo, and J.-y. Yang, Characteristic of adsorption, desorption, and co-transport of vanadium on humic acid colloid, *Ecotoxicology and Environmental Safety,* vol. 190, p. 110087, 2020.

[10] Z.-z. Wu, Y.-x. Zhang, J.-y. Yang, Y. Zhou, and C.-q. Wang, Effect of vanadium on testa, seed germination, and subsequent seedling growth of alfalfa (Medicago sativa L.), *Journal of Plant Growth Regulation,* vol. 40, no. 4, pp. 1566-1578, 2021.

[11] M. Imtiaz, M. S. Rizwan, S. Xiong, H. Li, M. Ashraf, S. M. Shahzad, M. Shahzad, M. Rizwan, and S. Tu, Vanadium, recent advancements and research prospects: A review, *Environment international,* vol. 80, pp. 79-88, 2015.

[12] M. M. Altaf, X.-p. Diao, M. A. Altaf, A. ur Rehman, A. Shakoor, L. U. Khan, B. L. Jan, and P. Ahmad, Silicon-mediated metabolic upregulation of ascorbate glutathione (AsA-GSH) and glyoxalase reduces the toxic effects of vanadium in rice, *Journal of Hazardous Materials,* vol. 436, p. 129145, 2022.

[13] M. A. Altaf, R. Shahid, M.-X. Ren, L. U. Khan, M. M. Altaf, M. S. Jahan, M. A. Nawaz, S. Naz, S. Shahid, and M. K. Lal, Protective mechanisms of melatonin against vanadium phytotoxicity in tomato seedlings: insights into nutritional status, photosynthesis, root architecture system, and antioxidant machinery, *Journal of Plant Growth Regulation,* vol. 41, no. 8, pp. 3300-3316, 2022.

[14] A. Aihemaiti, J. Jiang, Y. Gao, Y. Meng, Q. Zou, M. Yang, Y. Xu, S. Han, W. Yan, and T. Tuerhong, The effect of vanadium on essential element uptake of Setaria viridis' seedlings, *Journal of Environmental Management,* vol. 237, pp. 399-407, 2019.

[15] Z.-z. Wu, J.-y. Yang, Y.-x. Zhang, C.-q. Wang, S.-s. Guo, and Y.-q. Yu, Growth responses, accumulation, translocation and distribution of vanadium in tobacco and its potential in

phytoremediation, *Ecotoxicology and Environmental Safety,* vol. 207, p. 111297, 2021.
[16] N. Vachirapatama, Y. Jirakiattikul, G. Dicinoski, A. T. Townsend, and P. R. Haddad, Effect of vanadium on plant growth and its accumulation in plant tissues, *Sonklanakarin Journal of Science and Technology,* vol. 33, no. 3, p. 255, 2011.
[17] M. Imtiaz, M. S. Rizwan, M. A. Mushtaq, B. Yousaf, M. Ashraf, M. Ali, A. Yousuf, M. Rizwan, M. Din, and Z. Dai, Interactive effects of vanadium and phosphorus on their uptake, growth and heat shock proteins in chickpea genotypes under hydroponic conditions, *Environmental and Experimental Botany,* vol. 134, pp. 72-81, 2017.
[18] S. K. Ghosh, R. Saha, and B. Saha, Toxicity of inorganic vanadium compounds, *Research on Chemical Intermediates,* vol. 41, no. 7, pp. 4873-4897, 2015.
[19] D. Khan, X. Yang, G. He, R. A. A. Khan, B. Usman, L. Hui, A. A. Khokhar, Q. U. Zaman, and H.-F. Wang, Comparative physiological and transcriptomics profiling provides integrated insight into melatonin mediated salt and copper stress tolerance in Selenicereus undatus L, *Plants,* vol. 13, no. 24, p. 3602, 2024.
[20] S. U. Rahman, Y. Li, S. Hussain, B. Hussain, W.-u.-D. Khan, L. Riaz, M. N. Ashraf, M. A. Khaliq, Z. Du, and H. Cheng, Role of phytohormones in heavy metal tolerance in plants: A review, *Ecological Indicators,* vol. 146, p. 109844, 2023.
[21] Y. Pan, X. Xu, L. Li, Q. Sun, Q. Wang, H. Huang, Z. Tong, and J. Zhang, Melatonin-mediated development and abiotic stress tolerance in plants, *Frontiers in Plant Science,* vol. 14, p. 1100827, 2023.
[22] A. B. Lerner, J. D. Case, Y. Takahashi, T. H. Lee, and W. Mori, Isolation of melatonin, the pineal gland factor that lightens melanocyteS1, *Journal of the american chemical society,* vol. 80, no. 10, pp. 2587-2587, 1958.
[23] M. Niazi Khogeh, M. Rezaei, and Z. Ghasimi Hagh, Effect of salicylic acid and melatonin on chlorophyll fluorescence and initial growth of greenhouse tomatoes in salinity stress, *Journal of Plant Production Research,* vol. 29, no. 2, pp. 265-282, 2022.
[24] M. B. Arnao and J. Hernández-Ruiz, Melatonin: a new plant hormone and/or a plant master regulator?, *Trends in Plant Science,* vol. 24, no. 1, pp. 38-48, 2019.
[25] M. A. Altaf, R. Shahid, M.-X. Ren, M. M. Altaf, L. U. Khan, S. Shahid, and M. S. Jahan, Melatonin alleviates salt damage in tomato seedling: A root architecture system, photosynthetic capacity, ion homeostasis, and antioxidant enzymes analysis, *Scientia Horticulturae,* vol. 285, p. 110145, 2021.
[26] F. Yan, H. Wei, Y. Ding, W. Li, Z. Liu, L. Chen, S. Tang, C. Ding, Y. Jiang, and G. Li, Melatonin regulates antioxidant strategy in response to continuous salt stress in rice seedlings, *Plant Physiology and Biochemistry,* vol. 165, pp. 239-250, 2021.
[27] G. Zhao, Y. Zhao, X. Yu, F. Kiprotich, H. Han, R. Guan, R. Wang, and W. Shen, Nitric oxide is required for melatonin-enhanced tolerance against salinity stress in rapeseed (Brassica napus L.) seedlings, *International Journal of Molecular Sciences,* vol. 19, no. 7, p. 1912, 2018.
[28] M. H. Siddiqui, S. Alamri, M. Y. Al-Khaishany, M. N. Khan, A. Al-Amri, H. M. Ali, I. A. Alaraidh, and A. A. Alsahli, Exogenous melatonin counteracts NaCl-induced damage by regulating the antioxidant system, proline and carbohydrates metabolism in tomato seedlings, *International Journal of Molecular Sciences,* vol. 20, no. 2, p. 353, 2019.
[29] W. Wei, Q.-T. Li, Y.-N. Chu, R. J. Reiter, X.-M. Yu, D.-H. Zhu, W.-K. Zhang, B. Ma, Q. Lin, and J.-S. Zhang, Melatonin enhances plant growth and abiotic stress tolerance in soybean plants, *Journal of experimental botany,* vol. 66, no. 3, pp. 695-707, 2015.
[30] C. Jia, X. Yu, M. Zhang, Z. Liu, P. Zou, J. Ma, and Y. Xu, Application of melatonin-enhanced tolerance to high-temperature stress in cherry radish (Raphanus sativus L. var. radculus pers), *Journal of Plant Growth Regulation,* vol. 39, no. 2, pp. 631-640, 2020.
[31] R. K. Tiwari, M. K. Lal, R. Kumar, K. N. Chourasia, K. C. Naga, D. Kumar, S. K. Das, and G. Zinta, Mechanistic insights on melatonin-mediated drought stress mitigation in plants, *Physiologia Plantarum,* vol. 172, no. 2, pp. 1212-1226, 2021.
[32] M. A. Altaf, R. Shahid, M.-X. Ren, S. Naz, M. M. Altaf, L. U. Khan, R. K. Tiwari, M. K. Lal, M. A. Shahid, and R. Kumar, Melatonin improves drought stress tolerance of tomato by modulating

plant growth, root architecture, photosynthesis, and antioxidant defense system, *Antioxidants,* vol. 11, no. 2, p. 309, 2022.

[33] C. Kaya, M. Okant, F. Ugurlar, M. N. Alyemeni, M. Ashraf, and P. Ahmad, Melatonin-mediated nitric oxide improves tolerance to cadmium toxicity by reducing oxidative stress in wheat plants, *Chemosphere,* vol. 225, pp. 627-638, 2019.

[34] B. Debnath, A. Sikdar, S. Islam, K. Hasan, M. Li, and D. Qiu, Physiological and molecular responses to acid rain stress in plants and the impact of melatonin, glutathione and silicon in the amendment of plant acid rain stress, *Molecules,* vol. 26, no. 4, p. 862, 2021.

[35] D. Arnon and D. Hoagland, The investigation of plant nutrition by artificial culture methods, *Biological Reviews,* vol. 19, no. 2, pp. 55-67, 1944.

[36] M. Sengupta, A. Chakraborty, and S. S. Raychaudhuri, Ionizing radiation induced changes in phenotype, photosynthetic pigments and free polyamine levels in Vigna radiata (L.) Wilczek, *Applied Radiation and Isotopes,* vol. 75, pp. 44-49, 2013.

[37] H. K. Lichtenthaler, [34] Chlorophylls and carotenoids: pigments of photosynthetic biomembranes, in *Methods in enzymology*, vol. 148: Elsevier, 1987, pp. 350-382.

[38] A. R. Wellburn, The spectral determination of chlorophylls a and b, as well as total carotenoids, using various solvents with spectrophotometers of different resolution, *Journal of plant physiology,* vol. 144, no. 3, pp. 307-313, 1994.

[39] U. Schreiber, U. Schliwa, and W. Bilger, Continuous recording of photochemical and non-photochemical chlorophyll fluorescence quenching with a new type of modulation fluorometer, *Photosynthesis research,* vol. 10, no. 1, pp. 51-62, 1986.

[40] Q. W. Tan, P. K. Lim, Z. Chen, A. Pasha, N. Provart, M. Arend, Z. Nikoloski, and M. Mutwil, Cross-stress gene expression atlas of Marchantia polymorpha reveals the hierarchy and regulatory principles of abiotic stress responses, *Nature communications,* vol. 14, no. 1, p. 986, 2023.

[41] S. I. Zandalinas, Y. Fichman, A. R. Devireddy, S. Sengupta, R. K. Azad, and R. Mittler, Systemic signaling during abiotic stress combination in plants, *Proceedings of the National Academy of Sciences,* vol. 117, no. 24, pp. 13810-13820, 2020.

[42] P. Langfelder and S. Horvath, WGCNA: an R package for weighted correlation network analysis, *BMC bioinformatics,* vol. 9, no. 1, p. 559, 2008.

[43]H. Xia, Z. Ni, R. Hu, L. Lin, H. Deng, J. Wang, Y. Tang, G. Sun, X. Wang, and H. Li, Melatonin alleviates drought stress by a non-enzymatic and enzymatic antioxidative system in kiwifruit seedlings, *International journal of molecular sciences,* vol. 21, no. 3, p. 852, 2020.

[44] H. Yang, L. Dai, Y. Wei, Z. Deng, and D. Li, Melatonin enhances salt stress tolerance in rubber tree (Hevea brasiliensis) seedlings, *Industrial crops and products,* vol. 145, p. 111990, 2020.

[45] A. Zaid, F. Mohammad, S. H. Wani, and K. M. Siddique, Salicylic acid enhances nickel stress tolerance by up-regulating antioxidant defense and glyoxalase systems in mustard plants, *Ecotoxicology and environmental safety,* vol. 180, pp. 575-587, 2019.

[46] M. Rezayian, V. Niknam, and H. Ebrahimzadeh, Effects of drought stress on the seedling growth, development, and metabolic activity in different cultivars of canola, *Soil Science and Plant Nutrition,* vol. 64, no. 3, pp. 360-369, 2018.

[47] W.-y. He, W. Liao, J.-y. Yang, P. Jeyakumar, and C. Anderson, Removal of vanadium from aquatic environment using phosphoric acid modified rice straw, *Bioremediation Journal,* vol. 24, no. 1, pp. 80-89, 2020.

[48] A. R. Mir, J. Pichtel, and S. Hayat, Copper: uptake, toxicity and tolerance in plants and management of Cu-contaminated soil, *Biometals,* vol. 34, no. 4, pp. 737-759, 2021.

[49] M. S. Jahan, Y. Wang, S. Shu, M. Zhong, Z. Chen, J. Wu, J. Sun, and S. Guo, Exogenous salicylic acid increases the heat tolerance in Tomato (Solanum lycopersicum L) by enhancing photosynthesis efficiency and improving antioxidant defense system through scavenging of reactive oxygen species, *Scientia Horticulturae,* vol. 247, pp. 421-429, 2019.

[50] W. Cheng, A. Luo, H. Li, Z. Chen, Z. Guan, V. H. Escalona, D. Liu, Y. n. Zhou, F. Zhang, and Z. Huang, Variation in nutritional qualities and antioxidant capacity of different leaf mustard cultivars, *Horticulturae,* vol. 11, no. 1, p. 59, 2025.

[51] Q. Huang, H. Yan, M. You, J. Duan, M. Chen, Y. Xing, X. Hu, and X. Li, Enhancing drought tolerance and fruit characteristics in tomato through exogenous melatonin application, *Horticulturae,* vol. 9, no. 10, p. 1083, 2023.

[52] L. Yang, S. Bu, S. Zhao, N. Wang, J. Xiao, F. He, and X. Gao, Transcriptome and physiological analysis of increase in drought stress tolerance by melatonin in tomato, *PLoS One,* vol. 17, no. 5, p. e0267594, 2022.

[53] M. Michałek, P. Ogrodowicz, M. Kempa, A. Kuczyńska, and K. Mikołajczak, Melatonin in crop plants: from biosynthesis through pleiotropic effects to enhanced stress resilience, *Journal of Applied Genetics,* pp. 1-21, 2025.

[54] C. Y. Tu, Y. Q. Gao, L. Zheng, J. W. Ma, R. F. Shen, and X. F. Zhu, Melatonin improves aluminum resistance in rice (Oryza Sativa) via a nitric oxide dependent pathway, *Plant Growth Regulation,* pp. 1-17, 2025.

[55] M. Ameen, A. Zafar, A. Mahmood, M. A. Zia, K. Kamran, M. M. Javaid, M. Yasin, and B. A. Khan, Melatonin as a master regulatory hormone for genetic responses to biotic and abiotic stresses in model plant Arabidopsis thaliana: a comprehensive review, *Functional Plant Biology,* vol. 51, no. 2, 2024.

[56] L. Li, X. Yan, J. Li, X. Wu, and X. Wang, Metabolome and transcriptome association analysis revealed key factors involved in melatonin mediated cadmium-stress tolerance in cotton, *Frontiers in Plant Science,* vol. 13, p. 995205, 2022.

[57] Q. Gu, C. Xie, S. Zhang, T. Zhou, N. Li, C. Xu, Z. Zhou, C. Wang, and Z. Chen, Transcriptomic analysis provides insights into the molecular mechanism of melatonin-mediated cadmium tolerance in Medicago sativa L, *Ecotoxicology and Environmental Safety,* vol. 278, p. 116411, 2024.

[58] S. Basharat, W. Saeed, S. Mubeen, L. U. Khan, S. Zhang, P. Liu, and M. Waseem, Exogenous Melatonin Regulates Hormone Signalling and Photosynthesis-Related Genes to Enhance Brassica napus. Yield: A Transcriptomic Perspective, *Journal of Pineal Research,* vol. 77, no. 5, p. e70077, 2025.

[59] R. Ren, Z. Cao, X. Ma, Z. Li, K. Zhao, D. Cao, Q. Ma, M. Hou, K. Zhao, and L. Zhang, Multi-Omics Analysis Reveals That AhNHL Contributes to Melatonin-Mediated Cadmium Tolerance in Peanut Plants, *Journal of Pineal Research,* vol. 77, no. 2, p. e70035, 2025.

[60] S. Sang, S. Tian, W. Xu, H. Shi, and B. Deng, Dual defense: melatonin simultaneously mitigates cadmium toxicity and southern blight in peanut, *Frontiers in Plant Science,* vol. 16, p. 1686151, 2025.

[61] A. Sami, F. Shah, M. Abdullah, X. Zhou, Y. Yan, Z. Zhu, and K. Zhou, Melatonin mitigates cadmium and aluminium toxicity through modulation of antioxidant potential in Brassica napus L, *Plant Biology,* vol. 22, no. 4, pp. 679-690, 2020.



Copyright: © 2026 by the author(s). Published by Inspire Science and Tech Publisher, Pakistan. This article is an open access article distributed under Creative Commons Attribution License (CC BY 4.0), visit https:// creativecommons.org/licenses/by/4.0/